Micro-engineered Architected Metamaterials for Cell and Tissue Engineering

Chenyan Wang[1,2#], Zacharias Vangelatos[3#], Costas P. Grigoropoulos[3], Zhen Ma[1,2]*

1 Department of Biomedical & Chemical Engineering, Syracuse University, Syracuse NY 13244
2 BioInspired Syracuse Institute for Material and Living Systems, Syracuse University, Syracuse NY 13244
3 Department of Mechanical Engineering, University of California, Berkeley, CA 94720

[#]These two authors contribute to this manuscript equally.

[*]Correspondence to Zhen Ma (zma112@syr.edu)

Abstract

Architected metamaterials are built upon the assembly of repeating cellular structures, exhibiting unprecedented mechanical properties attributed to the tunability of cellular geometries. They have demonstrated a wide range of applications in the optical and electromagnetic fields, and recently they are employed as advanced tissue engineering scaffolds. The microgeometry-driven strategy enlarges the design domain of scaffold features and enables more accurate manipulation of cell-material interactions. In this review, we introduce the most popular metamaterial designs in biomedical engineering and summarize their representative applications to fabricate *in vitro* models and *in vivo* implants. These studies validate the unique advantages of metamaterials in supporting mechanobiological studies and improving the functionality of tissue replacements. Nevertheless, the evolution of meta-biomaterials requires more detailed investigations of the relationship between structural designs and cell phenotypes as well as accurate theoretical models.

Keywords: Mechanical Metamaterials, Biomaterials, Tissue Engineering, Meta-Implants

Abbreviations

3D	Three-dimensional
2D	Two-dimensional
FEA	Finite element analysis
AM	Additive manufacturing
CAD	Computer-aided design
FDM	Fused deposition modeling
SLM	Selective laser melting
TPP	Two-photon polymerization
TPMS	Triply periodic minimal surfaces
MEMS	Micro-electromechanical system
MSCs	Mesenchymal stem cells
MEW	Melt electro writing
HUVECs	Human umbilical vein endothelial cells
BM-MSCs	Bone marrow derived mesenchymal stem cells
ALP	Alkaline phosphatase activity
NGF	Nerve growth factor
MI	Myocardial infarction
BMP2	Bone morphogenetic protein 2
GI	Gastrointestinal
PCL	Polycaprolactone
TRL	Thermo-responsive linkers
PEGDA	Polyethylene glycol diacrylate
GelMa	Gelatin methacryloyl
PLA	Polylactic acid
PU	Polyurethane
PE	Polyethylene

Introduction

Since the last decade, the scientific community has aimed to design materials and structures that possess properties far greater than their natural counterparts. The concept of *metamaterials* or *architected materials* has emerged based on geometrical and structural configurations that can offer unique properties. The optical and electromagnetic metamaterials demonstrate excellent capability to dictate how optical[1] and electromagnetic[2] waves propagate through the materials. Mechanical metamaterials associated with structural mechanics focus on how the mechanical responses can be tuned in the elastic, plastic, nonlinear elastic, and fracture domains[3]. Controlling the properties, such as auxeticity[4], isotropy[5], and fracture impedance[6] is of critical importance for bioimplants[7], composites[8], and even aerospace engineering[9]. The mechanical performance of the metamaterials is controlled by their basic building blocks, called *unit cells*[10], which can be designed with different geometrical parameters. The most predominant category is lattice structures[11–13], which are comprised of beam members tactically arranged in the three-dimensional (3D) domain. Lattice structures have been employed in every aspect of mechanical metamaterial design, because they can be easily fabricated at different length scales and easily analyzed based on beam theory. Another emerging category in two-dimensional (2D) metamaterials, plate lattices[14,15], are often used predominantly for bistable, origami[16,17], and kirigami[18] structures that can reconfigure on controlled shapes for wave propagation and densification.

In the field of tissue engineering, one of the main goals is to engineer the desired scaffold that can home cells and direct their functions. Mechanical metamaterials offer an opportunity to expand the forms of mechanical signals in a reproducible way, thus they can be utilized to fabricate advanced scaffolds to precisely tune the biological behaviors of cells and tissues. A new concept of "meta-biomaterial" has emerged, referring to the mechanical metamaterials with biomimicry properties that are barely found in conventional porous biomaterials[19]. For example, the skin tissue exhibits lower stiffness under small strains while higher stiffness under large deformation, which has been reproduced in auxetic metamaterials with negative Poisson's ratio[20]. The macroscopic auxeticity can be achieved by stacking microunits with different configurations, such as chiral, re-entrant, or rotating elements[21,22]. Their use in tissue engineering is largely dependent on the feasibility of fabrication, since the property integrity is ensured by the accurate microgeometry and the way of assembly[23]. Besides, other critical properties such as stiffness, should be modified based on different applications. In another case, the trabecular bones possess both high strength and porosity, but these contradictory properties are very challenging to be engineered within the same biomaterial scaffold[24]. Such unique mechanical properties have been realized in metamaterials through the manipulation of their microscopic geometries. In addition to the advanced properties, mechanical metamaterials also show predictable mechanical behaviors based on their well-organized cellular units. Finite element analysis (FEA) is the most widely used tool in the simulation of stress distribution within metamaterials under external force[25–27]. In the metamaterial scaffolds populated by biological cells, cell-generated traction force can be analyzed based on the local strain analysis, which in turn, can further influence the cellular behaviors.

Nowadays, advanced manufacturing (AM) techniques have been used to generate nanoscopic patterns on metamaterials with high complexity[28]. The superior mechanical properties of metamaterial scaffolds are enabled by reliable AM techniques allowing 3D patterning of microscopic geometries guided by computer-aided design (CAD). Extrusion-based printing, especially fused deposition modeling (FDM), can continuously deposit melted polymer filaments to a supporting plate until the completion of 3D architected scaffolds[29], but the spatial resolution of printed cellular units is limited. The major advantages of FDM are the general material compatibility and the possibility of depositing multiple materials[28]. More structural complexity can be achieved by the employment of selective laser melting (SLM), which is based on the local laser sintering of a thin solid powder layer to generate designed patterns at predefined locations[30]. It has been used to create delicate penta-mode metamaterials with gradient diameters in their double-cone struts[31]. Selective laser sintering is simple and versatile in the use of a broad range of powders to produce porous ceramics and polymers to enhance bone regeneration in the fabricated tissues and permeating the growth of blood vessels[32]. One of the main challenges of this technique is to obtain the ideal fabrication conditions, such as the laser power and scanning speed. For polymers, the range of the glass transition temperature and melting temperature can result in substantial variations in the volume change of the scaffold[33]. Another prevalent technique, electron beam melting, utilizes an electron beam to selectively melt the powder bed[34]. The high velocity and a high beam power enable the design of high-performance alloys used in implant design. Thus, it has been employed for the realization of arbitrary open-cellular architectures[35]. Similar to the SLM, the effect of electron beam on the microstructure, the residual stresses and the material consolidation require fine control to provide the optimal result [36]. Binder jetting method is a cost-efficient technique that dispenses a liquid binding agent on a powder bed to create two-dimensional layers[37]. While it has been successfully employed for the design of lattice structures[38], the capillary pressure-wetting saturation between the agent and the powder may lead to non-uniformities in the porosity of the material.Multi-photon absorption occurring at the focal point of ultrafast lasers enables the production of ultrafine patterns when polymer resin is cured[39]. As an example, using the combination of two-photon polymerization (TPP) and oxygen-plasma etching, a lattice strut with a thickness at 19 nm has been fabricated, resulting in 60 times decrease of relative density compared to other materials with the similar topology and length scale[40]. However, the slow laser writing speed and limited field of view of high NA objective restrict the construction of mm scale structures[28]. All of these pros and cons need to be evaluated to select the most appropriate fabrication technique that can facilitate the required porosity, uniformity and material rigidity for the effective design of biological scaffolds possessing metamaterial structures.

In this review, we first introduce the current popular choices of mechanical metamaterials regarding their superior properties and the mechanisms of which microgeometries lead to these advantages. Then we summarize their current *in vitro* or *in vivo* applications in tissue engineering (**Table 1**). At last, we outlook future advances of metamaterials and emphasize the need of further investigations in different aspects to improve the practice of metamaterials in mechanobiological studies.

Cellular designs of metamaterials in biomedical applications

The most thoroughly studied mechanical metamaterials are ultra-light and ultra-stiff metamaterials[8,41–43], which have high strength at extremely low relative density. For the lattice structures, this ultra-light and ultra-stiff property can be accomplished by controlling the nodal connectivity between the structural beam members[11,13,44,45]. The number of beam members that share the same node determines whether the metamaterial is a bending or stretching dominating structure. Bending dominating structures can encompass higher strain energy density, due to the large deformation and densification of bending beams under compression. For stretching dominating structures, the higher nodal rigidity enables higher stiffness and higher yield strength. The determining factor distinguishing these two structures is the average connectivity Z[46], which is related to the number of beam members and nodes. The choice of unit cell with defined average connectivity is one of the design criteria to create a mechanical metamaterial for the applications of either energy absorption devices or ultra-stiff materials.

Apart from the implementation of different designs with defined average connectivity, such as the octet truss[13], cuboctahedron[47], Kelvin foam[48,49], diamond[47] , and Weaire-Phelan structure[47], it is critical to identify the anisotropy of metamaterial structures[5,11,50–52]. Anisotropy determines the variance in the elastic or plastic properties of the material at different loading directions[6,44]. This effect has a significant impact on the stress concentration on the structures, which may cause early failure and catastrophic collapse. To quantify the anisotropy of structures, the 3D polar stiffness map needs to be calculated and plotted numerically[11,50,51]. Since most metamaterial designs possess cubic symmetry, anisotropy index A is often used as a measure to quantify the anisotropy[4,8]. Controlling the anisotropy for metamaterial structures is crucial for the applications that require a smooth transition of stiffness gradient, such as bioimplants to avoid stress shielding[54] or wave mechanics to control the slope of the dispersion curves[55].

The auxetic architectures have been identified as a prevalent design candidate for biological applications. In nature, biological tissues are known to display auxetic characteristics, reported in skin[4], arteries, tendons, and cancellous bone[56]. Auxetic porous materials have been predicted to facilitate mass transport, which gives them a great potential for the delivery of nutrients and therapeutic agents, as well as the removal of metabolic wastes. The fundamental principle of auxetic structures is to overcome the volumetric Poisson effect through unique architected designs[57,58]. While the feasible range of Poisson's ratio is between -1 and 0.5, bulk materials without any specific microarchitectures usually do not have a negative value. Different classes of the auxetic metamaterials reveal a macroscopic negative Poisson effect under deformation, which would obstruct necking, barrel shape formation and catastrophic collapse of the material at a high deformation. The auxetic metamaterials can be designed as either re-entrant structures made of lattices[59], chiral models, or bucklicrystals comprised of grooved shell-resembling members[60]. Re-entrant unit cells possess hexagonal elements that can deform through the interior of the structure, leading to an auxetic behavior in the linear elastic domain[59,61]. Chiral units are formed by straight ribs connecting tangentially to central nodes, and the ribs will rotate in opposite directions depending on compression or stretch[62]. In contrast, bucklicrystals enable the auxeticity by controlling the buckling modes, which can direct the deformation field to the interior[63,64].

On the other hand, non-auxetic structures are mostly bending-dominated architectures, like diamond and rhombic dodecahedron, which leads to a critical deformation under mechanical compression. Diamond unit is made up by 16 equal edges and 14 vertices, and each node is connected to four others with an interior angle of 109.5°[65]. This large connection angle is the main reason of strut bending, in comparison to the buckling mode of cube unit struts (interior angle: 90°) in parallel to the loading direction, which could improve the compliance of biomaterials under mechanical force[66,67]. Moreover, the combination of auxetic and non-auxetic structures with an optimized structural gradient could provide a moderate mechanical strength and smooth internal stress transition, which can be engineered as the next generation of tissue engineering scaffolds.

Inspired by biological membranes and block copolymers, nanolabyrinth structures are designed to comprise triply periodic minimal surfaces (TPMS) that possess symmetries of a crystallographic group[68]. These surface designs, such as Schwarz P ("*Primitive*"), Schwarz D ("*Diamond*"), and Schwarz G ("*Gyroid*"), can locally minimize the surface area for a given boundary to achieve zero mean curvature at each point on the surface. In comparison to the lattice geometries, the smooth surfaces mitigate stress concentration and hinder catastrophic collapse in the structure[69]. More importantly, they can be employed to tailor the anisotropic behaviors, rendering the structures compliant in specific directions but extremely stiff at others. The anisotropic properties of nanolabyrinth structures make them feasible candidates for bioimplants and ultra-light structures. In addition, due to the shell elements within the structure, nanolabyrinth metamaterials demonstrate the capability to sustain large buckling deformation in a reversible manner. While this response is related to the shell buckling, the inherent complexity of this structure makes it difficult for further mechanical investigations from an analytical perspective.

The new applications of soft robotics, artificial muscles, and micro-electromechanical systems (MEMS) require large but reversible deformations. Since the photoresist materials used in microfabrication have a limited degree of elastic deformation, it is necessary to design architected structures to furnish this effect. To achieve hyper-elasticity and reversibility, structural bistability has been reported to contain multiple stable and unstable equilibrium positions, enabling it to transition between different deformation states. This bistability mechanism can be achieved by curved beam members or hinge design to allow the structures to transition from one equilibrium position to another. Specifically in the hinge design, 3D tensegrity structures with rigid beam members can reconfigure in 3D space through the rotation of the hinges. These tensegrity metamaterials have shown great potentials in wave propagation[70], transfer and storage of mechanical work[71], and controllable motion[72]. Furthermore, compliant metamaterials facilitate large irreversible deformation by connecting the beam members with hinges that are either free to rotate or have small resistance. Therefore, the structure can reconfigure to different geometries kinematically without the instigation of instability. Characteristic examples are origami[73] and kirigami[74] structures that have demonstrated nonreciprocal behaviors, control wave propagation, and tailored densification mechanisms.

Metamaterials for *in vitro* biological models

Natural or synthetic material scaffolds have been used to create the appropriate environment for different cell and tissue types[75–77]. The mechanical properties of scaffolds could be modified by changing either bulk property or porosity. In the case of laser-fabricated polymer scaffolds, the mechanical stiffness could be easily tuned by varying the ratio of crosslinkers and monomers or the laser processing intensity[78,79]. For these 3D printed scaffolds, the design of pore size and density can be precisely controlled in a layer-by-layer manner[80,81]. Bulk manufacturing techniques such as pore leaching[82], freeze drying[83] and electrospinning[84], are also widely used for making porous scaffolds at high efficiency. Nevertheless, it is still difficult to produce the scaffolds with high mechanical versatility due to the limited design space when the bulk property is predefined by the nature of polymers. The yield strength of commercially available synthetic polymers is within the range of 10 to 10^2 MPa with a density around 10^3, while the nickel lattice could provide a strength from 10^{-1} to 10^3 MPa, and the density could be extended to 10-10^4[85].The rational geometric designs of mechanical metamaterial scaffolds largely broaden the complexity of mechanical microenvironments, which is of great importance to mechanobiology studies that aim to correlate cell or tissue remodeling with mechanical designs in a quantitative way. In this section, we summarize *in vitro* biological models built upon the usage of metamaterials with tunable mechanical properties (**Figure 1**).

Metamaterials with tunable Poisson's ratio

Auxetic structures are the most popular metamaterials for tissue engineering applications because of their ability to direct unique cellular behaviors due to their negative Poisson's ratio. In an early study, embryonic fibroblasts were found to deform the laser-made auxetic webs to a large extent, while the web with positive Poisson's ratio showed a very limited deformation[86]. In turn, auxetic webs resulted in abnormal cell division, manifested as the failure of daughter cell separation. To manipulate single cells at a sub-cellular level, an auxetic cantilever was fabricated by deep reactive ion etching to obtain cellular units with a high aspect ratio and nanoscopic resolution[87] (**Figure 1A**). By growing the mesenchymal stem cells (MSCs) on either re-entrant or chiral structures, the cells exhibited linear or moon-like morphology in contrast to rounded or star-shaped morphology on coverslips. These MSCs tried to clime upon the auxetic structures instead of falling through the holes, because the surface adhesion force was stronger than the gravitational force. In addition, cell attachment caused the deformation of the auxetic structures and induced a shift of their resonant frequency, which can be used as a sensor for cell growth. In another study, C2C12 myoblasts demonstrated efficient muscle differentiation on the elastic auxetic micro-scaffolds fabricated by TPP. Myotubes fused on these scaffolds showed active actuations under a bipolar pulsed field stimulation[88].

Cells exert compressive traction force on the auxetic metamaterials, leading to local densification of their cellular units. This property not only reinforces the material scaffolds under mechanical load but also facilitates the formation of tight intercellular connections for 3D tissue assembly. Employing TPP, auxetic scaffolds with two different pore sizes were fabricated to support the 3D culture of fibroblasts[89]. Cells could only penetrate the scaffolds with larger pore sizes and modulate their orientation according to the directionality of the auxetic units. A mesenchymal microtissue model was established by seeding MSCs on both octet truss and auxetic metamaterials with a high density[90] (**Figure 1B**). On the octet truss structures, MSCs elongated and separated by the struts as individual cells, while auxetic structures promoted cell aggregation and tissue formation. In addition, FEA simulation showed that deformation patterns for the metamaterials under biological load were quite different from the deformation under common mechanical loading tests. A technique called melt electro writing (MEW), was used to deposit polymeric fibers with well-defined geometry and tunability of Poisson's ratio to fabricate the scaffolds for efficient tissue engineering applications[91] (**Figure 1C**). The thick fiber backbone defined the shape of cellular units and the auxetic behaviors, while the thin fiber web intertwining within each unit cell promoted cell growth. Human umbilical vein endothelial cells (HUVECs) tended to wrap around the fibers, while bone marrow stem cells were prone to fill the pores, which illustrated the distinct responses of different cell types to the auxetic webs.

Metamaterials with tunable porosity and stiffness

Porosity is one of the most essential design parameters for architected scaffolds, since it has a significant impact on cell behaviors and mass transport. For example, MSCs on the scaffolds with diamond crystal units and gradient density showed a higher alkaline phosphatase activity (ALP), which is an early marker of osteoblast differentiation, though all the scaffolds resulted in similar morphology, viability, and proliferation rate for MSC culture[92]. The uniqueness of this diamond crystal design was that low porosity at the inner layer of the scaffolds allowed more cell attachment, while high porosity at the outer layer promoted better cell proliferation and prevented the occurrence of pore occlusion. To better correlate the scaffold porosity and cellular behaviors, simulation-aided designs of gyroid lattices were fabricated by SLM[93] (**Figure 1D**). It was found that an increase of permeability due to high porosity was the main factor that promoted cell proliferation. During cell adhesion at the beginning, a lower cell number was observed on the scaffolds with larger pores. However, high permeability due to larger pore sizes enabled faster transport of nutrients and oxygen, which eventually promoted the rapid growth of cells within the scaffolds. It has also been shown that the upper limit of cell density can be optimized based on the balance between surface area and permeability of the scaffolds.

Manipulation of scaffold stiffness is important for mechanobiological studies under diverse mechanical environments. Although the stiffness of conventional materials can be easily tuned by varying the composition or architectures, it would inevitably change other mechanical properties of the scaffolds, such as porosity. It is difficult to independently investigate the influence of mechanical stiffness on cellular behaviors. The stiffness of metamaterial scaffolds can be modulated through the alteration of their microscopic geometries without affecting other properties. For example, 3D nanolattice scaffolds consisting of tetrakaidekahedral units were printed at high accuracy using TPP[94] **(Figure 1E)**. The struts radius and hollowness of individual units were varied to endow the scaffolds with different stiffness ranging from 0.7 MPa to 100 MPa but the same pore size. The osteoblast-like cells on the most compliant nanolattice produced more intracellular F-actin and minerals than the cells on the stiffer scaffolds. Based on these results, a model was established to describe the relationship between scaffold stiffness and actin concentration, which could further optimize the scaffold stiffness for maximal actin production and bone cell growth. Another work successfully decoupled the mass transport efficiency and the mechanical properties of penta-mode metamaterial scaffolds using various strut parameters[95]. The unique strut designs resulted in the transformation of material deformation patterns under the compressive load, thus the shear modulus was no longer negatively correlated with the volume fraction. Moreover, double-cone strut morphology increased the tortuosity of the scaffold surface and improved nutrient transport and waste removal. The simulation results of scaffold permeability showed a clear linear relationship with the experimental measurements, making it possible to predict the scaffold permeability based on the strut geometry.

To create metamaterial scaffolds that fulfill the requirements for different tissue engineering applications, a parametric optimization method was introduced to design TPMS sheet scaffolds composed of three different cellular geometries, including primitive, gyroid, and diamond, with defined porosity, Young's modulus, and pore sizes[96] **(Figure 1F)**. Based on the report of tissue-specific mechanical properties, the authors have optimized the cellular dimensions of metamaterials scaffolds to match with a variety of soft and hard tissues. This optimization method can also be employed to design new scaffolds with nonuniform mechanical properties by assembling two base materials with different Young's modulus. Stem cells cultured on the scaffolds might differentiate into multiple lineages directed by the mechanical heterogeneity. Moreover, the structural gradient present within native tissues, such as the zonal cartilage, could be simulated by combining primitive structures with various cellular dimensions or stacking primitive, gyroid, and diamond structures in a specialized order.

Metamaterials for engineered tissue implants

Metamaterials are promising scaffold candidates for tissue implants, because they can provide an in vivo-mimicking environment for endogenous cells and potentially minimize the immune responses. Their macroscopic mechanical flexibility enables them to adapt to various native environments, while their microscopic patterns offer topological guidance to cells, which may improve tissue function and regeneration. For the purpose of minimally invasive delivery, injectable hydrogels have been used for transplanting live cells to the injured site, but low cell viability due to extensive flow during injection dramatically reduces their therapeutic efficacy[97,98]. To solve this issue, compressible metamaterials have been explored for their macroscopic ductility enabling minimally invasive injection and sturdy microstructures that can protect the encapsulated cells from external mechanical stress. In this section, we discuss the use of metamaterials for tissue implants with different *in vivo* objectives (**Figure 2**).

Meta-implants for soft tissues

The deformability and fracture resistance of auxetic structures demonstrate significant advantages for engineering elastic patches for soft tissue regeneration. The extrusion-based bioprinting enabled the fabrication of a neural cell-laden auxetic patch that could bear the tensile force up to 20% strain[99]. Encapsulated Schwann's cells experiencing cyclic stretch showed the enhancement of cell viability, proliferation rate, and nerve growth factor (NGF) production than the cells under static culture. The excellent elasticity and degradability of the auxetic patch might play a synergistic effect on its superior functionality in neural tissue regeneration. The human heart is one of the most mechanically active organs, thus it's critical to create cardiac patches that can sustain the dynamic mechanical load. To resolve this challenge, a micropatterned auxetic patch was designed with re-entrant honeycombs[100] **(Figure 2A)**. By changing the dimensions of cellular units, the mechanical property of the auxetic patch can be modified to match the mechanical strength and structural anisotropy of the myocardium. *Ex vivo* results showed that auxetic patches were able to conform to the heart movements. After transplanting in a rat model with myocardial infarction (MI), the patch had a great integration with the left heart ventricle and resulted in negligible fibrotic responses. By two weeks, a significant increase of left ventricle mass was observed from the MI rats with the patch implants, which were hypothesized to decrease the heart wall stress and attenuate the hypertrophy. Four isometric crystal lattices as subtypes of body-centered cubic and face-centered cubic have been used as the basic building blocks of breast implants by taking advantage of their ideal symmetry and isotropy. Printed by FDM, the scaffolds with a ~90% porosity could support a large volume of fat tissue infiltration after implantation[101] **(Figure 2B)**. They also demonstrated excellent shape recovery after several compression cycles. The compressive mechanical test showed that the scaffolds with diamond lattice structures were the softest among all the designs, giving the best match with native breast tissues. After implanting the scaffolds into a nude rat model, softer scaffolds displayed a better performance than the stiffer scaffolds, demonstrated by promoting adipocyte survival, enhancing vascularization, and prohibiting fibrosis.

Meta-implants for hard tissues

The mechanical mismatch between the orthopedic implants and the native bone tissues often leads to stress-shielding, implant loosening, chronic immune responses, and final implant failure. The incorporation of meta-structures into medical implants enables superior mechanical properties that can potentially slow down the deterioration of orthopedic implants to improve their longevity. Early work has demonstrated the effect of different cell topologies on *in vivo* tissue regeneration in a canine model. The octet truss structure induced a faster rate of bone tissue ingrowth than the tetrahedron structure, although they both showed high mechanical strength for load-bearing applications[102]. Later on, the Zadpoor group highlighted the advantages of metamaterials by incorporating a mixture of cellular structures with negative and positive Poisson's ratios into a hip implant[103] **(Figure 2C)**. Unlike common implants that retract from one side of the interface, this hybrid meta-implant produced bilateral compressive force into surrounding bone tissues. This uniform compression increased the bone-implant contact, which would enhance the implant fixation and inhibit the entrance of wear particles. Moreover, the external compression and porous structures of the meta-implants stimulated bone ingrowth and regeneration.

Deformability is also introduced into stiff hard tissue implants to improve the surface compliance under a high mechanical force. A critical-sized acetabular bone defect frequently occurs during the total hip replacement surgery due to severe bone deficiencies. Common filling biomaterials do not have the perfect mechanical strength and shape to match such defects, which makes these filling materials difficult to stabilize and provide long-term support. Metamaterial scaffolds with a high positive Poisson's ratio can undergo a profound lateral expansion under compression, which makes them promising materials for this application. As a result, 3D-printed acetabular cup meta-implants based on several designs of non-auxetic structures with different densities were fabricated to have a large deformation without any mechanical failure[67] **(Figure 2D)**. By evaluating the deformation patterns of these space-filling meta-implants using load-displacement curves and microCT images, it has been found that the diamond metamaterials with a gradient density created the most desired deformation at the implant-mold interface compared to other designs.

In addition to modifications of mechanical properties, biofunctionalization of the lattice surface could further amplify the efficiency of tissue integration and regeneration. However, the complex topology of metamaterial makes it hard to have a uniform coating of bioactive molecules by physical deposition. TPMS have been largely used for bone tissue regeneration due to their feature of zero mean surface curvature resembling the trabecular bones. To obtain a tight molecular conjugation on the TPMS, a radical-rich polymeric coating was formed on the surface of Ti meta-implants using plasma polymerization and plasma immersion ion implantation[104]. This activated implant exhibited improved stability in corrosive solutions and promoted the immobilization of bone morphogenetic protein 2 (BMP2) for bone tissue growth. Zadpoor group demonstrated a layer-by-layer functionalization process to coat the metamaterial surface with antibiotic vancomycin and BMP2 in a consecutive manner[105]. Functionalized metamaterials showed a sustainable release of these two molecules for several weeks, and the release profile could be adjusted by switching the coating order of different chemicals. *In vitro* characterization showed that this meta-biomaterial had a strong antimicrobial performance and promoted the osteogenic differentiation of MSCs. *In vivo* assessment based on a rat model revealed that the transplantation would not induce a foreign body reaction, and the biofunctionalization facilitated the ingrowth of connective tissues to the metamaterial scaffolds.

Meta-implants for minimally invasive delivery

In 2006, the first origami pattern was adopted to fabricate self-deployable stent grafts using shape memory alloys to achieve minimally invasive delivery. The hill-valley patterns on the alloy foil allowed it to be folded to a small volume and inserted into an acrylic tube with a 13 mm radius, and then expanded to fill a 25 mm tube triggered by the temperature[106]. This early study gave rise to the subsequent development of injectable metamaterials as medical devices or drug carriers. Guided by the extensive mechanical simulation, a novel injectable meta-biomaterial was made by clustering irregular microparticles based on the cryogelation of carboxymethylcellulose to create a porous structure[107] **(Figure 2E)**. Compared to traditional microgels in which the porosity is limited to the interspace between particles, this meta-biomaterial showed an unprecedented elastic-softening transition given by multi-scale porosity and particle friction. This property made it possible for material injectability, *in situ* shaping capability, and matching the shear modulus to the surrounding tissues. Bone marrow stromal cells were seeded to the scaffolds after biofunctionalization for cell delivery applications. *In vivo* characterization in a mouse model showed that this meta-biomaterial scaffold had the ability to support cell growth and recruit endogenous tissues.

Deployable meta-implants with multi-stability can achieve minimal invasiveness during implantation[108]. Based on the rational arrangement of two basic bistable elements and four types of element connections, five deployable meta-implants were fabricated and tested for their stability at both deployment and retraction states with different mechanical loads. Among these meta-implants, auxetic units were the most appealing structures for minimizing tissue damage, because they had the smallest dimensions at their retraction configurations. Inspired by the Russian dolls, a multi-layer deployable meta-implant was fabricated based on the combination of kirigami and origami[109] **(Figure 2F)**. Bistability was introduced into the kirigami cuts on the flat sheets as 2D surface micropatterning. Based on the origami design, the meta-implants could be assembled with a uniform 3D surface functionality. Through the control of the number of layers, it was possible to adjust the mechanical properties and geometries of the implants.

Hierarchical metamaterials with a high surface area and flexible shape transformations can be used as efficient drug delivery vehicles. The rational design of the internal structural organization allows precise control of the drug release profile. A temperature-responsive deployable metamaterial composite was generated to deliver drugs to the gastrointestinal (GI) tract[110]. This composite was composed of three components: polycaprolactone (PCL) arms to bind the drugs, elastic hinges to provide the shape flexibility, and thermo-responsive linkers (TRLs) to disassemble the structure. Two drugs, carbamazepine, and moxifloxacin, were loaded to the folded metamaterial composite and administrated to a porcine model. Radiographic examination confirmed that the macrostructure deployed successfully in the stomach, remained intact under gastric contraction, and provided a sustained drug release for 2 weeks. This macrostructure could be disassembled by weakening the TRLs with 55°C water, and subsequently removed through the intestine without any obstruction. In another study, a kirigami-inspired drug delivery stent was made by inserting a soft actuator into a cylindrical shell, which consisted of an array of triangular cuts mimicking the patterns of snake skin[111]. This device could be made into a range of sizes to fit into different tubular organs, such as the GI tract, vasculature, and airways. The pressurized fluid would trigger the expansion of the actuator and erupt the triangular cuts, which could penetrate the esophageal tissue to release the drug microparticles. Only after a few minutes, this device could be transformed back to its original flat shape and removed by reducing the fluid pressure, while the drug microparticles were left inside the esophageal tissue for an extended release.

Conclusion and Future Perspectives

The application of metamaterials in tissue engineering is a representative demonstration of interdisciplinary research harnessing physical science, computational simulation, and mechanobiology. In comparison to traditional scaffolds on mechanical controls of cells and tissues, mechanical metamaterials possess significant advantages of refined cellular geometries and unprecedented mechanical properties. Many of their unique mechanical properties, such as extreme mechanical strength, negative Poisson's ratio, zero curvature, anisotropy, and deformability, have been utilized for *in vitro* and *in vivo* biomedical applications. Although the utility of metamaterials in biological studies has been well demonstrated, the variety of cellular designs used in cell and tissue engineering are relatively limited compared to the abundance of accessible geometries. Many other extraordinary mechanical properties found in metamaterials, such as negative compressibility, have not been widely applied in the biomedical fields yet. Dilatational metamaterials with 3D isotropic auxeticity have been printed at centimeter scales with extrusion printing and at micrometer scales using TPP, which can be used for creating a uniform tissue construct with multidirectional elasticity[112]. Due to the limitation of fabrication techniques, metamaterials with simpler microstructures were more often used for different applications. Further comparisons between the metamaterials with similar mechanical performances but different unit cell microstructures are needed. For example, both re-entrant and rotating rigid structures can provide the auxetic property, while the former is more frequently employed in the fabrication of tissue engineering scaffolds.

To ensure high fabrication resolution, metals and synthetic polymers are generally used for metamaterial fabrication, instead of natural biomaterials, which are too soft to maintain the structural integrity during 3D assembly. Loss of structural integrity makes it much more difficult for comparing different microgeometries and the matching their mechanical properties with theoretical predictions. Nevertheless, bioactivity and softness of natural biomaterials are essential for soft tissue engineering, thus future effort should be made towards the enhancement of their printability in the lattice fabrication. In addition to the advancement of fabrication techniques for natural soft materials, the combination of natural and synthetic materials could provide a great balance of mechanical strength and bioactivity. This could be achieved by mixing the polymer precursors to get uniform scaffolds, or generating natural-synthetic composites with spatial nonuniformity[113,114]. For example, the mechanical strength of gelatin and alginate hydrogels was improved by the dispersion of carbon nanofibers, which increased the shear-thinning and printability of the hybrid hydrogels when constructing a 3D lattice[115].

FEA modeling has been used extensively to guide new designs of metamaterial scaffolds and further enhance their mechanical functionalities. It has been well established to simulate the stress distribution within the metamaterials under external force, but the accuracy of FEA models reduces significantly when active cell-material interactions are taken into considerations for tissue engineering applications. The biological forces generated during tissue integration and remodeling are much more complex than the simulated force in FEA models. To optimize the FEA models, a composite system of tissue-metamaterial integration was simulated by incorporating a soft matrix that represented the bone tissue in the metamaterial scaffolds[116]. Hence, a new performance metric was established to evaluate the growth of bone tissue based on the strain field distribution within the soft matrix. The results showed that the spinodal shell topologies had better fatigue resistance and promoted more bone growth than the truss designs.

Using metamaterials as a platform for mechanobiology study is still at the early stage of development. The analysis of cell behaviors and responses on the metamaterials only emphasizes the morphological characterization of cell shape, attachment, and proliferation. The biological investigations still focus on how macroscopic mechanical properties of the metamaterial scaffolds influence cell and tissue phenotypes but lack in-depth studies on how microscopic unit structures affect cell remodeling. More molecular characterizations on cell metabolism, cytoskeleton organization, gene expression, and cell signaling will significantly advance our understanding of cell-material interactions based on the vast and precise metamaterial designs. For the applications of meta-implants, the design criteria need to be further refined for specific tissue types or disease conditions to improve their functionalities. To optimize the implants for minimally invasive delivery, the material degradation profile, external triggers for shape transformation, and surface biofunctionalization should be taken into considerations, in addition to the geometric design. Enhancement of tissue integration is especially important to the implants for long-term use, which requires more mechanistic understanding of cell-material interactions based on *in vitro* metamaterial model systems.

Acknowledgements
This work was supported by NSF (CBET-1804875, CBET-1804922, CBET-1943798, CMMI-2130192 and SNM-1449305) and Syracuse University intramural CUSE Grant.

Conflict of Interests
All authors declare no conflict of interest.

Figures and Captions

Table 1 Mechanical metamaterials and their applications in biomedical engineering

Category	Advantage in tissue engineering	Cellular Geometry	Material	Fabrication	Cellular response/Application	Reference
Auxetic	Negative and tunable Poisson's ratio, elastic, energy absorption, fracture resistance	Re-entrant	PEGDA	TPP	10T1/2 fibroblasts, movement, division	[86]
		Re-entrant, chiral	Negative photoresist	DIE	MSCs, attachment, migration	[87]
		Re-entrant	Negative photoresist	TPP	C2C12 muscle precursor cells, myotube formation	[88]
		Re-entrant	Organic-inorganic hybrid resin	TPP	3T3 fibroblasts, proliferation, penetration	[89]
		Re-entrant	Organic-inorganic hybrid resin	TPP	MSCs, 3D tissue assembly	[90]
		Re-entrant	PCL	MEW, FDM	HUVECs and BM-MSCs, attachment and growth	[91]
		Perforated sheet	GelMa	Moulding	Human Schwann cell, proliferation, differentiation	[99]
		Re-entrant	Chitosan	Laser microablation	Integrated cardiac patch	[100]
		Re-entrant	Ti6Al4V	SLM	Hybrid hip implant	[103]
Non-auxetic	Positive Poisson's ratio	Diamond, rhombic dodecahedron, cube truncated cube, truncated cuboctahedron, body-centered cube	Ti	3D printing	Space-filling implant	[67]
Ultra-stiff	Ultrahigh mechanical strength with large pore size, especially	Tetrahedron	Ti6AL4V	SLM	BM-MSCs, osteointegration and osteogenesis	[92]
		Tetrakaidecahedron	Negative photoresist	TPP	SAOS-2 cells,	[94]

	useful for hard tissue engineering				adhesion and mineralization	
		Double-cone elements	Ti6AL4V	SLM	Bone implant	[95]
		Tetrahedron, octet truss	Ti6AL4V	SLM	Bone implant	[102]
Isotropic	Symmetric structure, stackable units, tunable macroscopic mechanical property	Body-centered cubic, face-centered cubic	PU	3D printing	Elastic and compliant breast tissue implant	[101]
TPMS	Bone-like zero mean curvature	Diamond	Ti6Al4V	SLM	BM-MSCs, osteointegration and osteogenesis	[92]
		Gyroid	Stainless steel	SLM	Human Caucasian osteosarcoma cells, proliferation	[93]
		Primitive, gyroid, diamond	-	-	Natural tissue mimicking scaffold	[96]
		Diamond, gyroid	Ti	SLM	Bioactive bone implant	[104]
		Gyroid	Ti	SLM	Bone implant for dual drug release	[105]
Deployable	Shape flexibility	Origami	Shape memory alloy	Negative etching	Expandable vascular stents	[106]
		Fragmented porous particles	Carboxymethylcellulose	Cryogelation, fragmentation	Elastic, porous and injectable implants	[107]
		Bistable elements	PLA	FDM	Deployable implant	[108]
		Bistable elements, kirigami, origami	PLA, Al, Ti	Laser cutting	Deployable implant	[109]
		Arm, joint and linker assembly	Elastollan, PCL, PU	Moulding	Deployable drug delivery device	[110]
		Kirigami	PE	Laser cutting	Penetrative drug delivery device	[111]

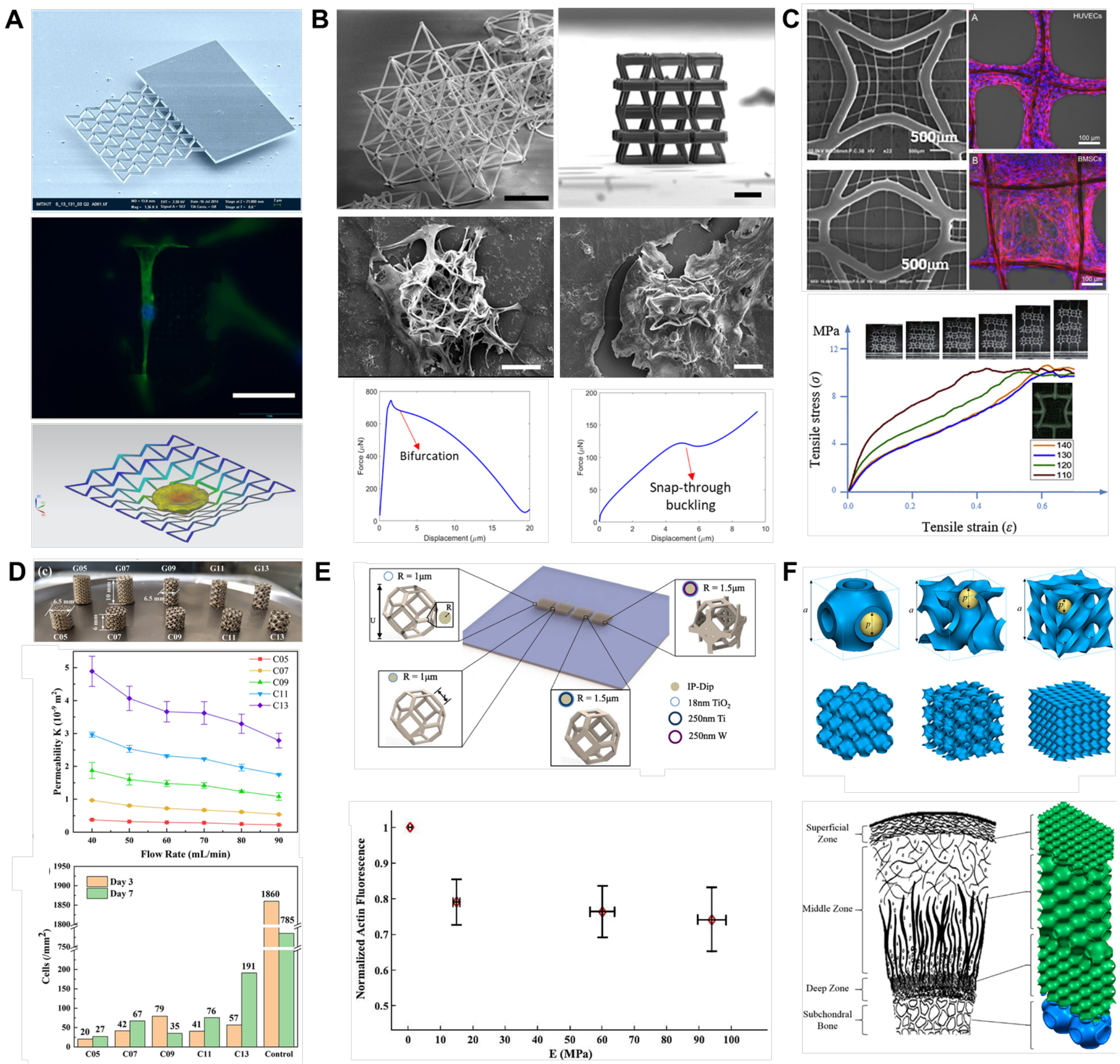

Figure 1. Metamaterial scaffolds with tunable mechanical properties for *in vitro* tissue engineering applications. (A) Auxetic cantilevers with a nanoscopic resolution were fabricated by deep reactive ion etching, and they showed a shift of resonant frequency when MSCs attached. Reprinted with permission from Ref. [87], Copyright (2015), IOP Publishing, Ltd. (B) Octet truss and auxetic lattices showed different deformation patterns under the mechanical load of mesenchymal microtissues. Reprinted with permission from Ref. [90], Copyright (2021), Mary Ann Liebert, Inc. (C) MEW enabled the fabrication of auxetic webs with tunable Poisson's ratio by intertwining thick and thin fibers. Bone marrow stem cells filled the large pores between thin fibers while vascular endothelial cells wrapped around the fibers. Reprinted with permission from Ref. [91], Copyright (2021), Elsevier. (D) Gyroid lattices with higher porosity and permeability inhibited the initial adhesion of human cancer cells but promoted cell proliferation in 7 days. Reprinted with permission from Ref. [93], Copyright (2020), Elsevier. (E) By varying the strut radius and hollowness of tetrakaidekahedral units, a huge range of stiffness magnitudes could be achieved with constant pore size. Based on the relationship between f-actin expression and scaffold stiffness, a phenomenological model was developed to guide the future design of bone scaffolds. Reprinted with permission from Ref. [94], Copyright (2017), Elsevier. (F) A parametric optimization method considering multiple mechanical parameters was established to direct the fabrication of TPMS metamaterial scaffolds with a better similarity to native tissues Reprinted with permission from Ref. [96], Copyright (2018), American Chemical Society.

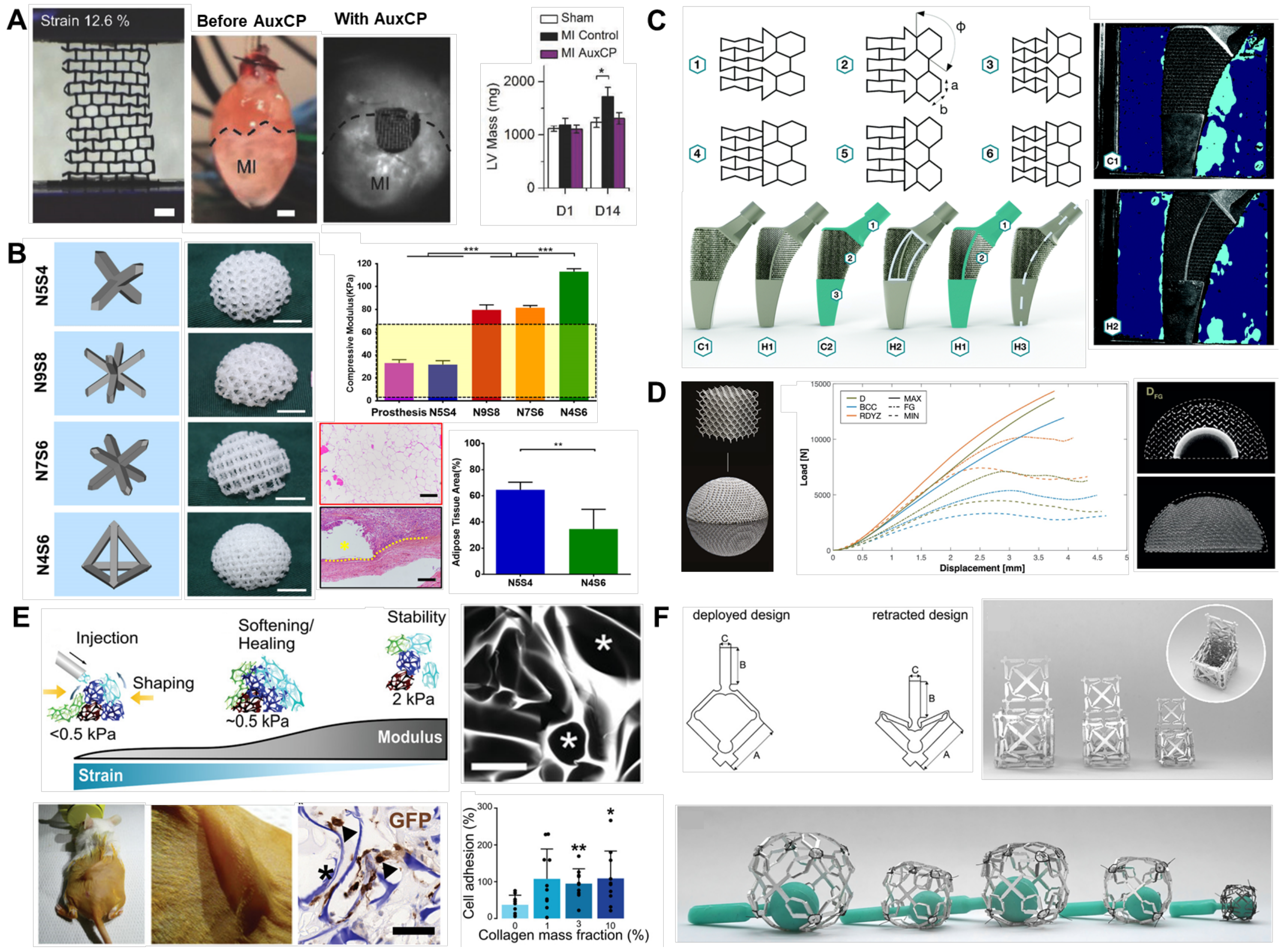

Figure 2. Metamaterial implants with superior mechanical properties for *in vivo* tissue support and minimally invasive delivery. (A) An auxetic cardiac patch with improved mechanical strength and anisotropy was created to improve its adaptivity to the heart movement during its beating, which might help to relieve the wall stress in the hypertrophic rat heart. Reprinted with permission from Ref. [100], Copyright (2018), John Wiley and Sons. (B) Four crystal lattices with different stiffness were used as the building blocks for breast tissue implants. The most compliant diamond structure provided the best mechanical match with the breast tissue and promoted the survival of adipose tissue after implantation in rats. Reprinted with permission from Ref. [101], Copyright (2019), IOP Publishing, Ltd. (C) A hybrid hip implant was manufactured leveraging the combination of cellular units with negative and positive Poisson's ratios. Its bilateral compression to surrounding tissues could improve the contact at their interface and the implant longevity. Reprinted with permission from Ref. [103], Copyright (2017), Royal Society of Chemistry. (D)Non-auxetic structures provided metamaterials with superior ductility that they had the potential to fulfill the critical-sized acetabular defect. Diamond structures with a gradient distribution manifested the most desired deformation at the implant-mold interface. Reprinted with permission from Ref. [67], Copyright (2021), Elsevier. (E) Elastic-softening transition was present in microgels composed of fragmented irregular particles, which enabled injectability, *in situ* shaping capability, and mechanical match with adjacent tissues in mice. This design could be generalized to serve as the cell delivery vehicle. Reprinted with permission from Ref. [107], Copyright (2021), John Wiley and Sons. (F) Bistability was utilized to fabricate origami-inspired deployable implants that provided a dramatic shape transformation triggered by the mechanical load. It could be assembled into multilayers to allow the adjustment of mechanical properties. Reprinted with permission from Ref. [109], Copyright (2020), Elsevier.

References:

[1] M. Schaeffer, G. Trainiti, M. Ruzzene, Optical Measurement of In-plane Waves in Mechanical Metamaterials Through Digital Image Correlation, Sci. Rep. 7 (2017) 42437. https://doi.org/10.1038/srep42437.

[2] Electromagnetic Metamaterials: Transmission Line Theory and Microwave Applications | IEEE eBooks | IEEE Xplore, (n.d.). https://ieeexplore.ieee.org/book/5237794 (accessed June 13, 2021).

[3] E. Barchiesi, M. Spagnuolo, L. Placidi, Mechanical metamaterials: a state of the art, Math. Mech. Solids. 24 (2019) 212–234. https://doi.org/10.1177/1081286517735695.

[4] A. Alderson, K.L. Alderson, Auxetic materials, Proc. Inst. Mech. Eng. Part G J. Aerosp. Eng. 221 (2007) 565–575. https://doi.org/10.1243/09544100JAERO185.

[5] X. Chen, J. Moughames, Q. Ji, J.A.I. Martínez, H. Tan, S. Adrar, N. Laforge, J.-M. Cote, S. Euphrasie, G. Ulliac, M. Kadic, V. Laude, Optimal isotropic, reusable truss lattice material with near-zero Poisson's ratio, Extreme Mech. Lett. 41 (2020) 101048. https://doi.org/10.1016/j.eml.2020.101048.

[6] M.R. O'Masta, L. Dong, L. St-Pierre, H.N.G. Wadley, V.S. Deshpande, The fracture toughness of octet-truss lattices, J. Mech. Phys. Solids. 98 (2017) 271–289. https://doi.org/10.1016/j.jmps.2016.09.009.

[7] G. Liu, Y. He, P. Liu, Z. Chen, X. Chen, L. Wan, Y. Li, J. Lu, Development of Bioimplants with 2D, 3D, and 4D Additive Manufacturing Materials, Engineering. 6 (2020) 1232–1243. https://doi.org/10.1016/j.eng.2020.04.015.

[8] J. Bauer, A. Schroer, R. Schwaiger, I. Tesari, C. Lange, L. Valdevit, O. Kraft, Push-to-pull tensile testing of ultra-strong nanoscale ceramic–polymer composites made by additive manufacturing, Extreme Mech. Lett. 3 (2015) 105–112. https://doi.org/10.1016/j.eml.2015.03.006.

[9] L. Hall, Ultralight Lattice-based Materials for Multifunctional Space Structure, NASA. (2018). http://www.nasa.gov/directorates/spacetech/esi/esi2017/Ultralight_Lattice-based_Materials (accessed August 26, 2021).

[10] J.U. Surjadi, L. Gao, H. Du, X. Li, X. Xiong, N.X. Fang, Y. Lu, Mechanical Metamaterials and Their Engineering Applications, Adv. Eng. Mater. 21 (2019) 1800864. https://doi.org/10.1002/adem.201800864.

[11] M. Abdelhamid, A. Czekanski, Impact of the Lattice Angle on the Effective Properties of the Octet-Truss Lattice Structure, J. Eng. Mater. Technol. 140 (2018). https://doi.org/10.1115/1.4040409.

[12] M. Alkhader, M. Nazzal, K. Louca, Design of bending dominated lattice architectures with improved stiffness using hierarchy, Proc. Inst. Mech. Eng. Part C J. Mech. Eng. Sci. 233 (2019) 3976–3993. https://doi.org/10.1177/0954406218810298.

[13] L.R. Meza, G.P. Phlipot, C.M. Portela, A. Maggi, L.C. Montemayor, A. Comella, D.M. Kochmann, J.R. Greer, Reexamining the mechanical property space of three-dimensional lattice architectures, Acta Mater. 140 (2017) 424–432. https://doi.org/10.1016/j.actamat.2017.08.052.

[14] C. Crook, J. Bauer, A. Guell Izard, C. Santos de Oliveira, J. Martins de Souza e Silva, J.B. Berger, L. Valdevit, Plate-nanolattices at the theoretical limit of stiffness and strength, Nat. Commun. 11 (2020) 1579. https://doi.org/10.1038/s41467-020-15434-2.

[15] T. Tancogne-Dejean, M. Diamantopoulou, M.B. Gorji, C. Bonatti, D. Mohr, 3D Plate-Lattices: An Emerging Class of Low-Density Metamaterial Exhibiting Optimal Isotropic Stiffness, Adv. Mater. 30 (2018) 1803334. https://doi.org/10.1002/adma.201803334.

[16] H. Yasuda, Y. Miyazawa, E.G. Charalampidis, C. Chong, P.G. Kevrekidis, J. Yang, Origami-based impact mitigation via rarefaction solitary wave creation, Sci. Adv. 5 (2019) eaau2835. https://doi.org/10.1126/sciadv.aau2835.

[17] F.S.L. Bobbert, S. Janbaz, T. van Manen, Y. Li, A.A. Zadpoor, Russian doll deployable meta-implants: Fusion of kirigami, origami, and multi-stability, Mater. Des. 191 (2020) 108624. https://doi.org/10.1016/j.matdes.2020.108624.
[18] T. Liu, S. Sun, H. Liu, N. An, J. Zhou, A predictive deep-learning approach for homogenization of auxetic kirigami metamaterials with randomly oriented cuts, Mod. Phys. Lett. B. 35 (2021) 2150033. https://doi.org/10.1142/S0217984921500330.
[19] A. A. Zadpoor, Meta-biomaterials, Biomater. Sci. 8 (2020) 18–38. https://doi.org/10.1039/C9BM01247H.
[20] X. Xin, L. Liu, Y. Liu, J. Leng, 4D printing auxetic metamaterials with tunable, programmable, and reconfigurable mechanical properties, Adv. Funct. Mater. 30 (2020) 2004226.
[21] X. Ren, R. Das, P. Tran, T.D. Ngo, Y.M. Xie, Auxetic metamaterials and structures: a review, Smart Mater. Struct. 27 (2018) 023001. https://doi.org/10.1088/1361-665X/aaa61c.
[22] P. Mardling, A. Alderson, N. Jordan-Mahy, C.L.L. Maitre, The use of auxetic materials in tissue engineering, Biomater. Sci. 8 (2020) 2074–2083. https://doi.org/10.1039/C9BM01928F.
[23] E. Dogan, A. Bhusal, B. Cecen, A.K. Miri, 3D Printing metamaterials towards tissue engineering, Appl. Mater. Today. 20 (2020) 100752.
[24] T.M. Keaveny, E.F. Morgan, G.L. Niebur, O.C. Yeh, Biomechanics of trabecular bone, Annu. Rev. Biomed. Eng. 3 (2001) 307–333.
[25] A. Rafsanjani, A. Akbarzadeh, D. Pasini, Snapping Mechanical Metamaterials under Tension, Adv. Mater. 27 (2015) 5931–5935. https://doi.org/10.1002/adma.201502809.
[26] W. Wu, D. Qi, H. Liao, G. Qian, L. Geng, Y. Niu, J. Liang, Deformation mechanism of innovative 3D chiral metamaterials, Sci. Rep. 8 (2018) 12575. https://doi.org/10.1038/s41598-018-30737-7.
[27] Z. Vangelatos, V. Melissinaki, M. Farsari, K. Komvopoulos, C. Grigoropoulos, Intertwined microlattices greatly enhance the performance of mechanical metamaterials, Math. Mech. Solids. 24 (2019) 2636–2648.
[28] M. Askari, D.A. Hutchins, P.J. Thomas, L. Astolfi, R.L. Watson, M. Abdi, M. Ricci, S. Laureti, L. Nie, S. Freear, Additive manufacturing of metamaterials: A review, Addit. Manuf. (2020) 101562.
[29] S.M. Montgomery, X. Kuang, C.D. Armstrong, H.J. Qi, Recent advances in additive manufacturing of active mechanical metamaterials, Curr. Opin. Solid State Mater. Sci. 24 (2020) 100869. https://doi.org/10.1016/j.cossms.2020.100869.
[30] A. Großmann, J. Gosmann, C. Mittelstedt, Lightweight lattice structures in selective laser melting: Design, fabrication and mechanical properties, Mater. Sci. Eng. A. 766 (2019) 138356. https://doi.org/10.1016/j.msea.2019.138356.
[31] R. Hedayati, A.M. Leeflang, A.A. Zadpoor, Additively manufactured metallic pentamode meta-materials, Appl. Phys. Lett. 110 (2017) 091905. https://doi.org/10.1063/1.4977561.
[32] S.F.S. Shirazi, S. Gharehkhani, M. Mehrali, H. Yarmand, H.S.C. Metselaar, N.A. Kadri, N.A.A. Osman, A review on powder-based additive manufacturing for tissue engineering: selective laser sintering and inkjet 3D printing, Sci. Technol. Adv. Mater. (2015).
[33] M. Schmid, A. Amado, K. Wegener, Polymer powders for selective laser sintering (SLS), in: AIP Publishing LLC, 2015: p. 160009.
[34] C. Körner, Additive manufacturing of metallic components by selective electron beam melting—a review, Int. Mater. Rev. 61 (2016) 361–377.
[35] F. Warmuth, F. Osmanlic, L. Adler, M.A. Lodes, C. Körner, Fabrication and characterisation of a fully auxetic 3D

lattice structure via selective electron beam melting, Smart Mater. Struct. 26 (2016) 025013.

[36] Q. Zhou, M.D. Hayat, G. Chen, S. Cai, X. Qu, H. Tang, P. Cao, Selective electron beam melting of NiTi: Microstructure, phase transformation and mechanical properties, Mater. Sci. Eng. A. 744 (2019) 290–298.

[37] M. Ziaee, N.B. Crane, Binder jetting: A review of process, materials, and methods, Addit. Manuf. 28 (2019) 781–801.

[38] L.A. Chavez, P. Ibave, B. Wilburn, D. Alexander, C. Stewart, R. Wicker, Y. Lin, The influence of printing parameters, post-processing, and testing conditions on the properties of binder jetting additive manufactured functional ceramics, Ceramics. 3 (2020) 65–77.

[39] E.C. Spivey, E.T. Ritschdorff, J.L. Connell, C.A. McLennon, C.E. Schmidt, J.B. Shear, Multiphoton Lithography of Unconstrained Three-Dimensional Protein Microstructures, Adv. Funct. Mater. 23 (2013) 333–339. https://doi.org/10.1002/adfm.201201465.

[40] A.J. Gross, K. Bertoldi, Additive Manufacturing of Nanostructures That Are Delicate, Complex, and Smaller than Ever, Small. 15 (2019) 1902370. https://doi.org/10.1002/smll.201902370.

[41] T.A. Schaedler, A.J. Jacobsen, A. Torrents, A.E. Sorensen, J. Lian, J.R. Greer, L. Valdevit, W.B. Carter, Ultralight Metallic Microlattices, Science. 334 (2011) 962–965. https://doi.org/10.1126/science.1211649.

[42] X. Zhang, A. Vyatskikh, H. Gao, J.R. Greer, X. Li, Lightweight, flaw-tolerant, and ultrastrong nanoarchitected carbon, Proc. Natl. Acad. Sci. 116 (2019) 6665–6672. https://doi.org/10.1073/pnas.1817309116.

[43] X. Wendy Gu, Julia.R. Greer, Ultra-strong architected Cu meso-lattices, Extreme Mech. Lett. 2 (2015) 7–14. https://doi.org/10.1016/j.eml.2015.01.006.

[44] V.S. Deshpande, N.A. Fleck, M.F. Ashby, Effective properties of the octet-truss lattice material, J. Mech. Phys. Solids. 49 (2001) 1747–1769. https://doi.org/10.1016/S0022-5096(01)00010-2.

[45] V.S. Deshpande, M.F. Ashby, N.A. Fleck, Foam topology: bending versus stretching dominated architectures, Acta Mater. 49 (2001) 1035–1040. https://doi.org/10.1016/S1359-6454(00)00379-7.

[46] Z. Vangelatos, K. Komvopoulos, J. Spanos, M. Farsari, C. Grigoropoulos, Anisotropic and curved lattice members enhance the structural integrity and mechanical performance of architected metamaterials, Int. J. Solids Struct. 193–194 (2020) 287–301. https://doi.org/10.1016/j.ijsolstr.2020.02.023.

[47] R. Hedayati, M. Sadighi, M. Mohammadi-Aghdam, A.A. Zadpoor, Effect of mass multiple counting on the elastic properties of open-cell regular porous biomaterials, Mater. Des. 89 (2016) 9–20. https://doi.org/10.1016/j.matdes.2015.09.052.

[48] L. Gong, S. Kyriakides, N. Triantafyllidis, On the stability of Kelvin cell foams under compressive loads, J. Mech. Phys. Solids. 53 (2005) 771–794. https://doi.org/10.1016/j.jmps.2004.10.007.

[49] W.-Y. Jang, S. Kyriakides, A.M. Kraynik, On the compressive strength of open-cell metal foams with Kelvin and random cell structures, Int. J. Solids Struct. 47 (2010) 2872–2883. https://doi.org/10.1016/j.ijsolstr.2010.06.014.

[50] S. Xu, J. Shen, S. Zhou, X. Huang, Y.M. Xie, Design of lattice structures with controlled anisotropy, Mater. Des. 93 (2016) 443–447. https://doi.org/10.1016/j.matdes.2016.01.007.

[51] W. Chen, S. Watts, J.A. Jackson, W.L. Smith, D.A. Tortorelli, C.M. Spadaccini, Stiff isotropic lattices beyond the Maxwell criterion, Sci. Adv. 5 (2019) eaaw1937. https://doi.org/10.1126/sciadv.aaw1937.

[52] Z. Vangelatos, C. Li, C. Grigoropoulos, K. Komvopoulos, Comparison of the mechanical performance of architected three-dimensional intertwined lattices at the macro/microscale, Extreme Mech. Lett. 40 (2020) 100930. https://doi.org/10.1016/j.eml.2020.100930.

[53] S.I. Ranganathan, M. Ostoja-Starzewski, Universal Elastic Anisotropy Index, Phys. Rev. Lett. 101 (2008) 055504.

https://doi.org/10.1103/PhysRevLett.101.055504.

[54] S. Vijayavenkataraman, A. Gopinath, W.F. Lu, A new design of 3D-printed orthopedic bone plates with auxetic structures to mitigate stress shielding and improve intra-operative bending, Bio-Des. Manuf. 3 (2020) 98–108. https://doi.org/10.1007/s42242-020-00066-8.

[55] X. Xia, A. Afshar, H. Yang, C.M. Portela, D.M. Kochmann, C.V. Di Leo, J.R. Greer, Electrochemically reconfigurable architected materials, Nature. 573 (2019) 205–213. https://doi.org/10.1038/s41586-019-1538-z.

[56] Y. Prawoto, Seeing auxetic materials from the mechanics point of view: A structural review on the negative Poisson's ratio, Comput. Mater. Sci. 58 (2012) 140–153. https://doi.org/10.1016/j.commatsci.2012.02.012.

[57] D. Attard, E. Manicaro, R. Gatt, J.N. Grima, On the properties of auxetic rotating stretching squares, Phys. Status Solidi B. 246 (2009) 2045–2054. https://doi.org/10.1002/pssb.200982035.

[58] A. Ingrole, A. Hao, R. Liang, Design and modeling of auxetic and hybrid honeycomb structures for in-plane property enhancement, Mater. Des. 117 (2017) 72–83. https://doi.org/10.1016/j.matdes.2016.12.067.

[59] M. Shokri Rad, Y. Prawoto, Z. Ahmad, Analytical solution and finite element approach to the 3D re-entrant structures of auxetic materials, Mech. Mater. 74 (2014) 76–87. https://doi.org/10.1016/j.mechmat.2014.03.012.

[60] S. Babaee, J. Shim, J.C. Weaver, E.R. Chen, N. Patel, K. Bertoldi, 3D Soft Metamaterials with Negative Poisson's Ratio, Adv. Mater. 25 (2013) 5044–5049. https://doi.org/10.1002/adma.201301986.

[61] L. Yang, O. Harrysson, H. West, D. Cormier, Mechanical properties of 3D re-entrant honeycomb auxetic structures realized via additive manufacturing, Int. J. Solids Struct. 69–70 (2015) 475–490. https://doi.org/10.1016/j.ijsolstr.2015.05.005.

[62] A. Alderson, K.L. Alderson, D. Attard, K.E. Evans, R. Gatt, J.N. Grima, W. Miller, N. Ravirala, C.W. Smith, K. Zied, Elastic constants of 3-, 4- and 6-connected chiral and anti-chiral honeycombs subject to uniaxial in-plane loading, Compos. Sci. Technol. 70 (2010) 1042–1048. https://doi.org/10.1016/j.compscitech.2009.07.009.

[63] S. Yuan, F. Shen, J. Bai, C.K. Chua, J. Wei, K. Zhou, 3D soft auxetic lattice structures fabricated by selective laser sintering: TPU powder evaluation and process optimization, Mater. Des. 120 (2017) 317–327. https://doi.org/10.1016/j.matdes.2017.01.098.

[64] F. Wang, Systematic design of 3D auxetic lattice materials with programmable Poisson's ratio for finite strains, J. Mech. Phys. Solids. 114 (2018) 303–318. https://doi.org/10.1016/j.jmps.2018.01.013.

[65] S. Ahmadi, G. Campoli, S.A. Yavari, B. Sajadi, R. Wauthlé, J. Schrooten, H. Weinans, A. Zadpoor, Mechanical behavior of regular open-cell porous biomaterials made of diamond lattice unit cells, J. Mech. Behav. Biomed. Mater. 34 (2014) 106–115.

[66] C.P. de Jonge, H.M.A. Kolken, A.A. Zadpoor, Non-Auxetic Mechanical Metamaterials, Materials. 12 (2019) 635. https://doi.org/10.3390/ma12040635.

[67] H. Kolken, C. de Jonge, T. van der Sloten, A.F. Garcia, B. Pouran, K. Willemsen, H. Weinans, A. Zadpoor, Additively manufactured space-filling meta-implants, Acta Biomater. 125 (2021) 345–357.

[68] A. Pressley, Gauss's Theorema Egregium, in: A. Pressley (Ed.), Elem. Differ. Geom., Springer, London, 2001: pp. 229–246. https://doi.org/10.1007/978-1-4471-3696-5_10.

[69] O. Al-Ketan, R. Rezgui, R. Rowshan, H. Du, N.X. Fang, R.K.A. Al-Rub, Microarchitected Stretching-Dominated Mechanical Metamaterials with Minimal Surface Topologies, Adv. Eng. Mater. 20 (2018) 1800029. https://doi.org/10.1002/adem.201800029.

[70] N. Nadkarni, C. Daraio, D.M. Kochmann, Dynamics of periodic mechanical structures containing bistable elastic elements: From elastic to solitary wave propagation, Phys. Rev. E. 90 (2014) 023204.

https://doi.org/10.1103/PhysRevE.90.023204.
[71] S. Fang, X. Fu, W.-H. Liao, Asymmetric plucking bistable energy harvester: Modeling and experimental validation, J. Sound Vib. 459 (2019) 114852. https://doi.org/10.1016/j.jsv.2019.114852.
[72] Y. Zhong, R. Du, L. Wu, H. Yu, A Novel Articulated Soft Robot Capable of Variable Stiffness through Bistable Structure, in: 2020 IEEE Int. Conf. Robot. Autom. ICRA, 2020: pp. 2939–2945. https://doi.org/10.1109/ICRA40945.2020.9197479.
[73] D. Melancon, B. Gorissen, C.J. García-Mora, C. Hoberman, K. Bertoldi, Multistable inflatable origami structures at the metre scale, Nature. 592 (2021) 545–550. https://doi.org/10.1038/s41586-021-03407-4.
[74] X. Zhang, L. Medina, H. Cai, V. Aksyuk, H.D. Espinosa, D. Lopez, Kirigami Engineering—Nanoscale Structures Exhibiting a Range of Controllable 3D Configurations, Adv. Mater. 33 (2021) 2005275. https://doi.org/10.1002/adma.202005275.
[75] J.J. Rice, M.M. Martino, L. De Laporte, F. Tortelli, P.S. Briquez, J.A. Hubbell, Engineering the regenerative microenvironment with biomaterials, Adv. Healthc. Mater. 2 (2013) 57–71.
[76] L. Gu, D.J. Mooney, Biomaterials and emerging anticancer therapeutics: engineering the microenvironment, Nat. Rev. Cancer. 16 (2016) 56–66.
[77] R.C. Bretherton, C.A. DeForest, The Art of Engineering Biomimetic Cellular Microenvironments, ACS Biomater. Sci. Eng. (2021).
[78] M. Dadsetan, J.P. Szatkowski, M.J. Yaszemski, L. Lu, Characterization of Photo-Cross-Linked Oligo[poly(ethylene glycol) fumarate] Hydrogels for Cartilage Tissue Engineering, Biomacromolecules. 8 (2007) 1702–1709. https://doi.org/10.1021/bm070052h.
[79] A. Dobos, J. Van Hoorick, W. Steiger, P. Gruber, M. Markovic, O.G. Andriotis, A. Rohatschek, P. Dubruel, P.J. Thurner, S. Van Vlierberghe, S. Baudis, A. Ovsianikov, Thiol–Gelatin–Norbornene Bioink for Laser-Based High-Definition Bioprinting, Adv. Healthc. Mater. 9 (2020) 1900752. https://doi.org/10.1002/adhm.201900752.
[80] S.A. Park, S.H. Lee, W.D. Kim, Fabrication of porous polycaprolactone/hydroxyapatite (PCL/HA) blend scaffolds using a 3D plotting system for bone tissue engineering, Bioprocess Biosyst. Eng. 34 (2011) 505–513.
[81] C. Shuai, Z. Mao, H. Lu, Y. Nie, H. Hu, S. Peng, Fabrication of porous polyvinyl alcohol scaffold for bone tissue engineering via selective laser sintering, Biofabrication. 5 (2013) 015014.
[82] J. Reignier, M.A. Huneault, Preparation of interconnected poly(ε-caprolactone) porous scaffolds by a combination of polymer and salt particulate leaching, Polymer. 47 (2006) 4703–4717. https://doi.org/10.1016/j.polymer.2006.04.029.
[83] A. Autissier, C. Le Visage, C. Pouzet, F. Chaubet, D. Letourneur, Fabrication of porous polysaccharide-based scaffolds using a combined freeze-drying/cross-linking process, Acta Biomater. 6 (2010) 3640–3648.
[84] A. Thorvaldsson, H. Stenhamre, P. Gatenholm, P. Walkenström, Electrospinning of highly porous scaffolds for cartilage regeneration, Biomacromolecules. 9 (2008) 1044–1049.
[85] T.A. Schaedler, W.B. Carter, Architected Cellular Materials, Annu. Rev. Mater. Res. 46 (2016) 187–210. https://doi.org/10.1146/annurev-matsci-070115-031624.
[86] W. Zhang, P. Soman, K. Meggs, X. Qu, S. Chen, Tuning the Poisson's Ratio of Biomaterials for Investigating Cellular Response, Adv. Funct. Mater. 23 (2013) 3226–3232. https://doi.org/10.1002/adfm.201202666.
[87] A.D. Lantada, A. Muslija, J.P. García-Ruíz, Auxetic tissue engineering scaffolds with nanometric features and resonances in the megahertz range, Smart Mater. Struct. 24 (2015) 055013. https://doi.org/10.1088/0964-1726/24/5/055013.

[88] M.R. Gullo, S. Takeuchi, O. Paul, Muscle-actuated bio-hybrid mems by cell culture and differentiation on me tamaterial micro-scaffolds, in: 2016 IEEE 29th Int. Conf. Micro Electro Mech. Syst. MEMS, 2016: pp. 721–724. https://doi.org/10.1109/MEMSYS.2016.7421729.

[89] G. Flamourakis, I. Spanos, Z. Vangelatos, P. Manganas, L. Papadimitriou, C. Grigoropoulos, A. Ranella, M. Farsari, Laser-made 3D Auxetic Metamaterial Scaffolds for Tissue Engineering Applications, Macromol. Mater. Eng. 305 (2020) 2000238. https://doi.org/10.1002/mame.202000238.

[90] C. Wang, Z. Vangelatos, T. Winston, S. Sun, C.P. Grigoropoulos, Z. Ma, Remodeling of Architected Mesenchymal Microtissues Generated on Mechanical Metamaterials, 3D Print. Addit. Manuf. (2021). https://doi.org/10.1089/3dp.2021.0091.

[91] Y. Jin, C. Xie, Q. Gao, X. Zhou, G. Li, J. Du, Y. He, Fabrication of multi-scale and tunable auxetic scaffolds for tissue engineering, Mater. Des. 197 (2021) 109277. https://doi.org/10.1016/j.matdes.2020.109277.

[92] H. Wang, K. Su, L. Su, P. Liang, P. Ji, C. Wang, The effect of 3D-printed Ti6Al4V scaffolds with various macropore structures on osteointegration and osteogenesis: A biomechanical evaluation, J. Mech. Behav. Biomed. Mater. 88 (2018) 488–496. https://doi.org/10.1016/j.jmbbm.2018.08.049.

[93] S. Ma, Q. Tang, X. Han, Q. Feng, J. Song, R. Setchi, Y. Liu, Y. Liu, A. Goulas, D.S. Engstrøm, Manufacturability, mechanical properties, mass-transport properties and biocompatibility of triply periodic minimal surface (TPMS) porous scaffolds fabricated by selective laser melting, Mater. Des. 195 (2020) 109034.

[94] A. Maggi, H. Li, J.R. Greer, Three-dimensional nano-architected scaffolds with tunable stiffness for efficient bone tissue growth, Acta Biomater. 63 (2017) 294–305. https://doi.org/10.1016/j.actbio.2017.09.007.

[95] L. Zhang, B. Song, L. Yang, Y. Shi, Tailored mechanical response and mass transport characteristic of selective laser melted porous metallic biomaterials for bone scaffolds, Acta Biomater. 112 (2020) 298–315.

[96] S. Vijayavenkataraman, L. Zhang, S. Zhang, J.Y. Hsi Fuh, W.F. Lu, Triply periodic minimal surfaces sheet scaffolds for tissue engineering applications: An optimization approach toward biomimetic scaffold design, ACS Appl. Bio Mater. 1 (2018) 259–269.

[97] B.A. Aguado, W. Mulyasasmita, J. Su, K.J. Lampe, S.C. Heilshorn, Improving viability of stem cells during syringe needle flow through the design of hydrogel cell carriers, Tissue Eng. Part A. 18 (2012) 806–815.

[98] A.A. Foster, L.M. Marquardt, S.C. Heilshorn, The diverse roles of hydrogel mechanics in injectable stem cell transplantation, Curr. Opin. Chem. Eng. 15 (2017) 15–23.

[99] Y.-W. Chen, K. Wang, C.-C. Ho, C.-T. Kao, H.Y. Ng, M.-Y. Shie, Cyclic tensile stimulation enrichment of Schwann cell-laden auxetic hydrogel scaffolds towards peripheral nerve tissue engineering, Mater. Des. 195 (2020) 108982. https://doi.org/10.1016/j.matdes.2020.108982.

[100] M. Kapnisi, C. Mansfield, C. Marijon, A.G. Guex, F. Perbellini, I. Bardi, E.J. Humphrey, J.L. Puetzer, D. Mawad, D.C. Koutsogeorgis, Auxetic cardiac patches with tunable mechanical and conductive properties toward treating myocardial infarction, Adv. Funct. Mater. 28 (2018) 1800618.

[101] M. Zhou, J. Hou, G. Zhang, C. Luo, Y. Zeng, S. Mou, P. Xiao, A. Zhong, Q. Yuan, J. Yang, Z. Wang, J. Sun, Tuning the mechanics of 3D-printed scaffolds by crystal lattice-like structural design for breast tissue engineering, Biofabrication. 12 (2019) 015023. https://doi.org/10.1088/1758-5090/ab52ea.

[102] S. Arabnejad, R. Burnett Johnston, J.A. Pura, B. Singh, M. Tanzer, D. Pasini, High-strength porous biomaterials for bone replacement: A strategy to assess the interplay between cell morphology, mechanical properties, bone ingrowth and manufacturing constraints, Acta Biomater. 30 (2016) 345–356. https://doi.org/10.1016/j.actbio.2015.10.048.

[103] H.M. A. Kolken, S. Janbaz, S.M. A. Leeflang, K. Lietaert, H. H. Weinans, A. A. Zadpoor, Rationally designed meta-implants: a combination of auxetic and conventional meta-biomaterials, Mater. Horiz. 5 (2018) 28–35. https://doi.org/10.1039/C7MH00699C.

[104] M. Croes, B. Akhavan, O. Sharifahmadian, H. Fan, R. Mertens, R.P. Tan, A. Chunara, A.A. Fadzil, S.G. Wise, M.C. Kruyt, A multifaceted biomimetic interface to improve the longevity of orthopedic implants, Acta Biomater. 110 (2020) 266–279.

[105] S.A. Yavari, M. Croes, B. Akhavan, F. Jahanmard, C. Eigenhuis, S. Dadbakhsh, H. Vogely, M. Bilek, A. Fluit, C. Boel, Layer by layer coating for bio-functionalization of additively manufactured meta-biomaterials, Addit. Manuf. 32 (2020) 100991.

[106] K. Kuribayashi, K. Tsuchiya, Z. You, D. Tomus, M. Umemoto, T. Ito, M. Sasaki, Self-deployable origami stent grafts as a biomedical application of Ni-rich TiNi shape memory alloy foil, Mater. Sci. Eng. A. 419 (2006) 131–137. https://doi.org/10.1016/j.msea.2005.12.016.

[107] A. Béduer, F. Bonini, C.A. Verheyen, M. Genta, M. Martins, J. Brefie-Guth, J. Tratwal, A. Filippova, P. Burch, O. Naveiras, An Injectable Meta-Biomaterial: From Design and Simulation to In Vivo Shaping and Tissue induction, Adv. Mater. (2021) 2102350.

[108] F.S. L. Bobbert, S. Janbaz, A. A. Zadpoor, Towards deployable meta-implants, J. Mater. Chem. B. 6 (2018) 3449–3455. https://doi.org/10.1039/C8TB00576A.

[109] F. Bobbert, S. Janbaz, T. van Manen, Y. Li, A. Zadpoor, Russian doll deployable meta-implants: Fusion of kirigami, origami, and multi-stability, Mater. Des. 191 (2020) 108624.

[110] S. Babaee, S. Pajovic, A.R. Kirtane, J. Shi, E. Caffarel-Salvador, K. Hess, J.E. Collins, S. Tamang, A.V. Wahane, A.M. Hayward, Temperature-responsive biometamaterials for gastrointestinal applications, Sci. Transl. Med. 11 (2019).

[111] S. Babaee, Y. Shi, S. Abbasalizadeh, S. Tamang, K. Hess, J.E. Collins, K. Ishida, A. Lopes, M. Williams, M. Albaghdadi, Kirigami-inspired stents for sustained local delivery of therapeutics, Nat. Mater. (2021) 1–8.

[112] T. Bückmann, R. Schittny, M. Thiel, M. Kadic, G.W. Milton, M. Wegener, On three-dimensional dilational elastic metamaterials, New J. Phys. 16 (2014) 033032. https://doi.org/10.1088/1367-2630/16/3/033032.

[113] F. Pati, J. Jang, D.-H. Ha, S.W. Kim, J.-W. Rhie, J.-H. Shim, D.-H. Kim, D.-W. Cho, Printing three-dimensional tissue analogues with decellularized extracellular matrix bioink, Nat. Commun. 5 (2014) 1–11.

[114] S. Hong, D. Sycks, H.F. Chan, S. Lin, G.P. Lopez, F. Guilak, K.W. Leong, X. Zhao, 3D printing of highly stretchable and tough hydrogels into complex, cellularized structures, Adv. Mater. 27 (2015) 4035–4040.

[115] A. Serafin, C. Murphy, M.C. Rubio, M.N. Collins, Printable alginate/gelatin hydrogel reinforced with carbon nanofibers as electrically conductive scaffolds for tissue engineering, Mater. Sci. Eng. C. 122 (2021) 111927. https://doi.org/10.1016/j.msec.2021.111927.

[116] M.-T. Hsieh, M.R. Begley, L. Valdevit, Architected implant designs for long bones: Advantages of minimal surface-based topologies, Mater. Des. 207 (2021) 109838.